Liquid Crystals
Publication details, including instructions for authors and subscription information:
http://www.informaworld.com/smpp/title~content=t713926090

Kinetics of the nematic phase growth across the isotropic-nematic phase transition in polymer-dispersed liquid crystals

Sergei Bronnikov[a]; Carmen Racles[b]; Vasile Cozan[b]
[a] Institute of Macromolecular Compounds, Sankt Petersburg, Russian Federation [b] 'Petru Poni' Institute of Macromolecular Chemistry, Iasi, Romania

To cite this Article Bronnikov, Sergei , Racles, Carmen and Cozan, Vasile(2009) 'Kinetics of the nematic phase growth across the isotropic-nematic phase transition in polymer-dispersed liquid crystals', Liquid Crystals, 36: 3, 319 — 328
To link to this Article: DOI: 10.1080/02678290902859390
URL: http://dx.doi.org/10.1080/02678290902859390

Liquid Crystals,
Vol. 36, No. 3, March 2009, 319–328

Taylor & Francis
Taylor & Francis Group

Kinetics of the nematic phase growth across the isotropic-nematic phase transition in polymer-dispersed liquid crystals

Sergei Bronnikov[a]*, Carmen Racles[b] and Vasile Cozan[b]

[a]*Institute of Macromolecular Compounds, Bolshoi Prospekt 31, Sankt Petersburg, 199004 Russian Federation;* [b]*'Petru Poni' Institute of Macromolecular Chemistry, Aleea Gr. Ghica Voda 41A, Iasi, 700487 Romania*

(Received 12 February 2009; final form 2 March 2009)

Polymer-dispersed liquid crystals (PDLCs) composed of poly(dimethyl siloxane), cured poly(dimethyl siloxane) and polysulfone (as matrices), and an azomethine compound (as an embedded mesogen varying in weight from 5 to 80%) were prepared via solvent-induced phase separation. After preparation, they were heated to the melt and then cooled; phase transitions upon both heating and cooling were detected with a differential scanning calorimeter and a polarising optical microscope (POM). The nematic droplets appearing in the POM images across the isotropic-nematic phase transition were treated statistically and described with principles of irreversible thermodynamics. Furthermore, kinetics of the nematic phase growth across this phase transition was studied and described analytically with the universal law for cluster growth. Both flexibility of the polymer matrix and the mesogen content in PDLCs were shown to influence the processes studied.

Keywords: polymer-dispersed liquid crystals; isotropic-nematic phase transition; nematic phase growth; polarising optical images

1. Introduction

Polymer-dispersed liquid crystals (PDLCs) represent an important new class of materials with electro-optic applications. PDLC is a mixture of liquid crystals (LCs) and monomer, in which phase separation is induced by either thermal/UV curing or solvent evaporation (*1–3*). The resulting two-phase system contains LC domains, usually in the forms of droplets, which are surrounded with a polymer matrix. The nematic texture within each LC domain is randomly oriented, so that incoming visible light is scattered, and the PDLC appears milky white. Application of an external (electromagnetic, thermal, mechanical, etc.) field causes orientation of domains in the preferred direction, and the PDLC becomes transparent if the refractive indexes of LCs and polymer are the same, or at least similar.

There are two principal methods of PDLC preparation: encapsulation and phase separation (*1–3*). In the first method, an LC is mixed with a polymer dissolved in water. When the water is evaporated, the LC is surrounded (encapsulated) by a polymer matrix. These LC capsules are non-uniform in size and tend towards coalescence. In the second method, an LC first is mixed with polymer/monomer. Consequently, LC domains are formed by the phase separation of the components. There are three methods of phase separation, namely monomer polymerisation, thermal action and solvent evaporation.

Polymerisation-induced phase separation occurs immediately when LC is mixed with a monomer solution. The LC domains grow until polymerisation finishes, i.e. when the polymer matrix becomes solid enough. Thermally induced phase separation (TIPS) occurs when the polymer matrix has a melting temperature below its decomposition temperature. First, LC is mixed with a melted polymer. Then the mixture is cooled at a specific rate to cause phase separation. While the polymer hardens, LC domains appear. They grow until the glass transition temperature is achieved. Solvent induced phase separation (SIPS) occurs when both LC and polymers dissolved in the same solvent are mixed. The solvent evaporation at a specific rate induces the phase separation. The growth of the LC domains stops when the solvent is removed entirely.

PDLCs are already widely used for manufacturing flat-panel displays, switchable windows, holographic films, etc. Nowadays PDLC displays with a very high resolution, near a laser printer quality, are produced. They are very bright because polarisers absorbing more than half of transmitted light are not needed. Also, PDLC films are easy to manufacture since their exact thickness is not important. Since phase transitions, phase separation, nucleation and the LC phase growth are important characteristics of PDLCs suitable for technical application, these phenomena are the focus of intensive research, both scientific and industrial.

A review of research publications of last 15 years reveals an increasing interest in PDLCs. The analysis

*Corresponding author. Email: sergei_bronnikov@yahoo.com

ISSN 0267-8292 print/ISSN 1366-5855 online

DOI: 10.1080/02678290902859390
http://www.informaworld.com

of structure, size, shape and packing of LC droplets embedded into the polymer matrix of PDLC seems to be very important, since these parameters directly affect the electro-optical behaviour of PDLCs (*2*, *4*, *5*). Much attention has also been paid to the morphological study of PDLCs (*5–10*). Kinetics of the phase separation in LC/monomer systems across thermally/UV power-induced polymerisation as a function of LC concentration, UV curing power and temperature have been experimentally studied (*4*, *6*, *7*, *11*) and simulated (*3*, *12*, *13*), though TIPS in isotropic (i.e., above their clearing point) LC embedded into polymer matrix and subjected to deep cooling is not studied in depth, except in one case (*7*).

We should emphasise here that in the references mentioned, the growing LC droplet size across the phase separation had not been subjected to statistical analysis, except in two cases (*10*, *11*). In (*5*), the mean droplet diameter was evaluated as 'the inverse square root of the number of drops intersecting the image plane divided by the image area'. Such evaluation should be treated as an approximate rather than an accurate one. Meanwhile, statistical treatment of optical images can give information on the LC droplet diameter distribution width and on the mean droplet diameter; both characteristics are important for technical application of PDLCs. Moreover, statistical analysis of multi-component LC mixtures can clarify compatibility/non-compatibility of the LC components in the mixture (*14*, *15*).

In this work, we report on kinetics of the ordered (nematic) phase growth across the isotropic–nematic (I–N) phase transition of the LC fraction dispersed into the polymer matrix of PDLC. For analytical description of the ordered phase growth across the phase separation of PDLCs we used the theory of phase-ordering kinetics (*16*), suitable for LC systems. Applicability of this theory to both mono- and multi-component LC systems in 2D space (thin layers of LCs) has been proved (*14*, *15*, *17–20*), though for strongly confined systems (an LC phase embedded into polymer matrix) such verifications have not been made. We expect a specific behaviour in such systems because of particularity of their structures. Indeed, upon PDLC formation, the polymer matrix, being a random confinement structure, subjects the embedded LC component to a random elastic stress depending on the polymer 'rigidity'. Due to extremely low inherent LC elasticity, this stress is expected to dramatically affect the LC phase ordering across the isotropic-nematic transition and the size of growing LC nuclei.

We will also show how the nature of the polymer matrix ('flexible', 'semi-flexible', and 'rigid') and concentration of LC phase influence the kinetics of the ordered phase growth.

2. Experimental

2.1 Materials

Many publications available for PDLCs report on the E7 commercial mesogen component (*6*, *10*, *11*). In the present study, we chose another, chemically simpler, azomethine mesogen compound, 4[4-chloro-phenylene-imino-methylidene-phenoxy-hexylene-oxy]-benzaldehyde, with higher transition temperatures (see below). Its chemical structure is presented in Figure 1. It was obtained in a two-step procedure: dibromohexane was reacted with *p*-hydroxybenzaldehyde and the resulted dialdehyde was reacted with *p*-chloroaniline.

Three polymers, namely, i) poly(dimethyl siloxane) (Pdms) with M_n = 40,000, ii) cross-linked poly (dimethyl siloxane) (PdmsE) and iii) Udel bisphenol A-polysulfone (PSF) with M_n = 38,000, were used as matrices when PDLCs were manufactured. Their chemical structures are also shown in Figure 1.

Pdms was obtained by the cation exchange catalysed ring-opening polymerisation of octamethylcyclotetrasiloxane. According to (*21*), we used tetraethylorthosilicate (TEOS) as a cross-linking agent in 2/1 weight ratio and dibutyltin dilaurate (DBTDL) as a catalyst for the Pdms curing.

2.2 Sample preparation

The PDLC samples were manufactured using combination of SIPS and TIPS. First, the LC and Pdms (or Pdms/TEOS 2/1 and a drop of DBTDL in the case of PdmsE series) were dissolved in tetrahydrofuran (THF) in the pre-established ratios. Then the solution was poured onto Petri dishes and some drops were placed on microscope slides for optical observations, where the solvent slowly evaporated at ambient conditions. In the case of PdmsE series, after 24h the samples were kept in the oven at 180°C for 1 h, to complete the cross-linking. In the case of PSF, the mixtures were prepared in a way similar to the Pdms series, except the polymer was dissolved in chloroform.

The following proportions of the LC component were imbedded into the polymer matrices: 5, 10, 20, 50 and 80 wt% (into both Pdms and PdmsE) and 20, 50 and 80 wt% (into PSF). Henceforth, we will designate the PDLCs investigated as an abbreviated polymer matrix name along with percentage of the LC component involved, e.g. Pdms50.

2.3 Measurements

The thermotropic behaviour of the neat LC and the LC/polymer systems was investigated by differential

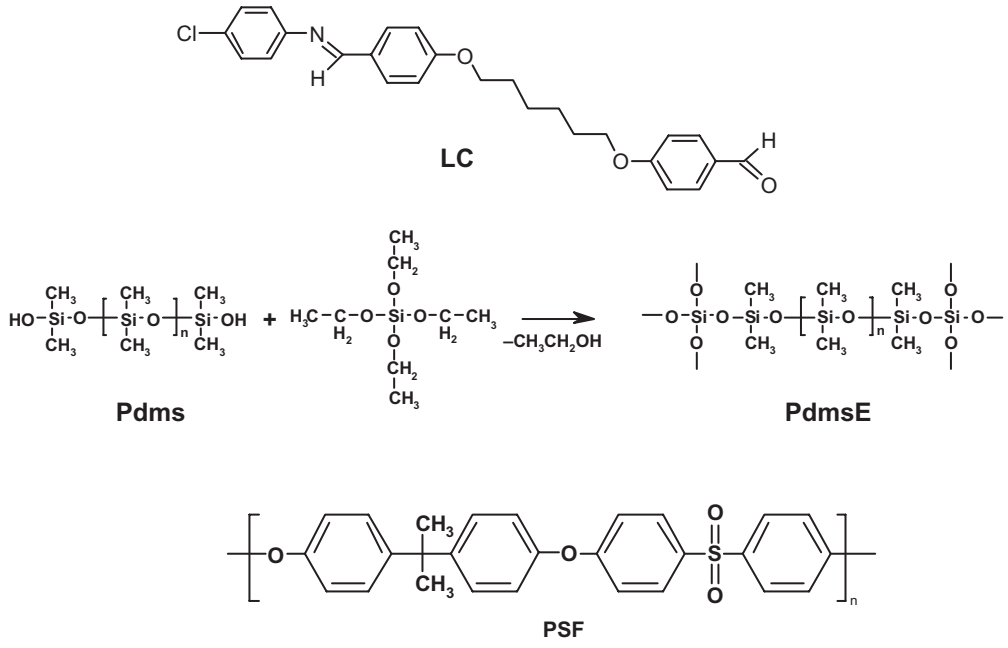

Figure 1. Chemical structures of the PDLCs' components including azomethine LC component and three polymer matrices: Pdms, PdmsE and PSF. In this figure, transformation (i.e. curing) of Pdms to PdmsE is also depicted.

scanning calorimetry (DSC) using a Pyrus Diamond power compensation Perkin Elmer instrument at both heating and cooling rates of 10°C min^{-1}, and by polarising optical microscopy (POM) using an Olympus BH-2 instrument fitted with a THMS 600/HSF9I hot stage and a digital camera attached to the ocular. For POM observations of the phase transitions, the samples were placed into a commercially available sandwich cell with a gap of 10 μm and consequently heated at 20°C min^{-1} to the isotropic state, kept for 10 min and cooled at 10°C min^{-1}. In the cooling regime, short movies were captured to identify the ordered phase nucleation and consequent growth across the I–N phase transition.

The optical images obtained were subsequently segmented and subjected to digital image analysis with the ImageTool 3.0 software (Health Science Center, the University of Texas, San Antonio, USA) to elucidate the statistical size distribution of nematic droplets. For analytical description of the resulting histograms, we used the model of reversible aggregation.

3. Model

The model of reversible aggregation (*22*, *23*) gives a general characterisation of micro-structure in liquid systems. According to the model, stationary non-equilibrium micro-structure is developed by linking the energy-equivalent dynamic units in metastable clusters called aggregates, which are permanently formed and decomposed under thermal fluctuations. By analogy with simultaneously and reversibly ongoing linear chemical reactions, the thermodynamic interpretation of the micro-structure evolution shows that the aggregation is controlled by the standard aggregation energy.

Since PDLCs were analysed within a planar boundary condition cell, we employed the equation describing the statistical size distribution of the micro-structural entities, in a 2D form. It is written as

$$h(s - s_0) = a(s - s_0)^2 \exp\left(-\frac{(s - s_0)\Delta u_0}{kT}\right), \qquad (1)$$

where s is the characteristic aggregate size, s_0 is a minimum (embryonic) aggregate size, a is a normalising parameter, Δu_0 is the aggregate energy, k is the Boltzmann constant and T is the absolute temperature. We chose the droplet area as a characteristic size s. Then the mean droplet area $<s>$ can be determined as the normalised mathematical expectation

$$\langle s \rangle = s_0 + \frac{\int_0^\infty sh(s)ds}{\int_0^\infty h(s)ds} = s_0 + \frac{3kT}{\Delta u_0}. \qquad (2)$$

Taking into account a circular form of the nematic droplets, the mean droplet diameter $<d>$ can be found as

$$\langle d \rangle = 2\left(\frac{s_0 + \langle s \rangle}{\pi}\right)^{\frac{1}{2}}. \quad (3)$$

4. Results and discussion

Table 1 lists the transition temperatures of PDLCs and LC upon both heating and cooling. A sequence of transitions in the neat LC component identified by DSC is presented, in comparison with that observed by POM. The transitions in the LC component of PDLCs were obtained from POM observations upon heating. We also present the starting temperature of the kinetic investigation, identified as the temperature at which the first droplets appeared upon cooling the isotropic melt. From the data obtained with DSC, we present only the glass transition temperatures, T_g, of the polymer matrices, since in many cases the energy of certain transitions in the LC phase was too weak to be detected accurately.

As follows from Table 1, the N–I transition temperatures detected upon heating and the I–N transition temperatures detected upon cooling are not the same in the most cases. The N–I transition was around 185°C, while the I–N transition was observed at lower temperatures, probably due to the difference in heating and cooling rates and also due to the effect of the polymeric matrix, which hindered the ordering of the LC component.

On the other hand, different effects on the polymers T_g were observed for 'flexible' (Pdms) and 'rigid' (PSF) matrices. No variations in T_g were registered for Pdms and PdmsE series (around −123°C), which supports the expected incompatibility and phase separation between two components of the mixtures. In the PSF mixtures, T_g was much lower than that of the neat polymer ($T_g \approx$185°C); this indicates the phase mixing. The miscibility of the PDLC components was shown to be an important parameter for LC dispersibility in a polymer matrix (*7*). However, a perfect miscibility would exclude the phase separation, thus the formation of the LC droplets. In our study, two different situations were realised. The LC/Pdms and LC/PdmsE systems are immiscible, which is reflected by a large difference in the solubility parameters: δ = 7.43 $cal^{1/2}$ $cm^{-3/2}$ for Pdms (*24*) and 10.7 $cal^{1/2}$ $cm^{-3/2}$ for LC, calculated with a Bicerano method (*25*). Conversely, the LC/PSF systems are miscible since the difference between the solubility parameters is very small: δ = 9.97 $cal^{1/2}$ $cm^{-3/2}$ for PSF (*24*) and 10.7 $cal^{1/2}$ $cm^{-3/2}$ for LC (*25*). The solvents also influence the miscibility of the components; their solubility parameters, equal to 9.21 $cal^{1/2}$ $cm^{-3/2}$ for chloroform and 9.52 $cal^{1/2}$ $cm^{-3/2}$ for THF) (*26*), sustain the phase separation tendency in both LC/Pdms and LC/PdmsE systems, and the enhanced miscibility in LC/PSF system. These peculiarities are confirmed by the thermal behaviour of the polymer matrices as described above.

In Figure 2, we present a combination of the DSC and POM data for selected PDLC samples upon both heating and cooling. Figure 2(a) gives the thermal and optical properties of Pdms50. According to the POM images, the melting upon heating started at 105°C, and a smectic (Sm) texture appeared gradually within a large temperature range; in the DSC curve, the melting was detected as a broad peak centred at 100°C. At 130°C, a weak transition was detected by DSC,

Table 1. Thermal behaviour of the LC/polymer systems investigated.

Sample code	Phase transitions in neat LC and glass transition in PDLC matrices obtained from DSC curves upon second heating at 20°C min^{-1}, °C	LC transitions obtained from POM observation upon heating at 20°C min^{-1}, °C	I–N transition obtained from POM observation upon cooling at 10°C min^{-1}*, °C
Neat LC	Cr–144–Sm–173–N–204–I	Cr–138–Sm–170–N–197–I	195
Pdms5	–123.5	Cr–158–LC–180–I	163.5
Pdms10	–123.5	Cr–145–N–187–I	182.5
Pdms20	–123.5	Cr–107–Sm–140–N–185–I	178
Pdms50	–123.5	Cr–105–Sm–146–N–183–I	183
Pdms80	–123.5	Cr–104–Sm–145–N–190–I	174
PdmsE5	–122.5	Cr–143–N–172–I	152
PdmsE10	–122.5	Cr–147–LC–170–I	155
PdmsE20	–122.8	Cr–150–N–185–I	150
PdmsE50	–122.5	Sm–120–N–183–I	173
PdmsE80	–122.8	Cr–150–N–181–I	166
PSF20	100	Cr–140–Sm–185–I	165
PSF50	85	Cr–155–N–202–I	200
PSF80	90	Cr–147–Sm–174–N–198	190

*Beginning of the statistical kinetic investigations.

which could not be assigned in POM. A Sm–N transition began at 146°C (POM data); this transition was centred at 160°C (DSC data). The nematic schlieren texture disappeared in the POM image at about 183°C; in the DSC curve, this isotropisation transition appeared as a shoulder.

Upon cooling, the I–N transition could not be detected by DSC, while in the POM image it started at 183°C. According to the microscopic observations, the nematic droplets coalesced and formed a continuous texture, which turned into the smectic texture at about 130°C, then slowly crystallised. In the DSC curve, two exothermal peaks were detected, at 157 and 114°C, which would correspond to the beginning of the N–Sm transition and to the crystallisation, respectively.

The DSC curve and the texture of PdmsE50 are depicted in Figure 2(b). The DSC curve upon heating showed numerous peaks; not all of them could be clearly identified in the POM observations, probably because the sample was blurred and at a higher magnification very small domains were visible. The first endotherms in the DSC curve could most probably be assigned to the melting (possible polymorphic); the asymmetric peak centred at 135°C could be due to the Sm–N transition, while that centred at 147°C would rather correspond to the isotropisation. Upon cooling, the only transition was detected at 107°C. All these transitions appeared in PdmsE at much lower temperatures than those in the neat LC, probably due to the previous thermal treatment and cross-linking of the sample. In the POM images obtained upon heating, the nematic texture was observed at 120°C, and the N–I transition was broad (from 158 to 183°C). Upon cooling, the I–N transition began at 173°C. A smectic texture was observed at 140°C, and the sample crystallisation was detected at 109°C.

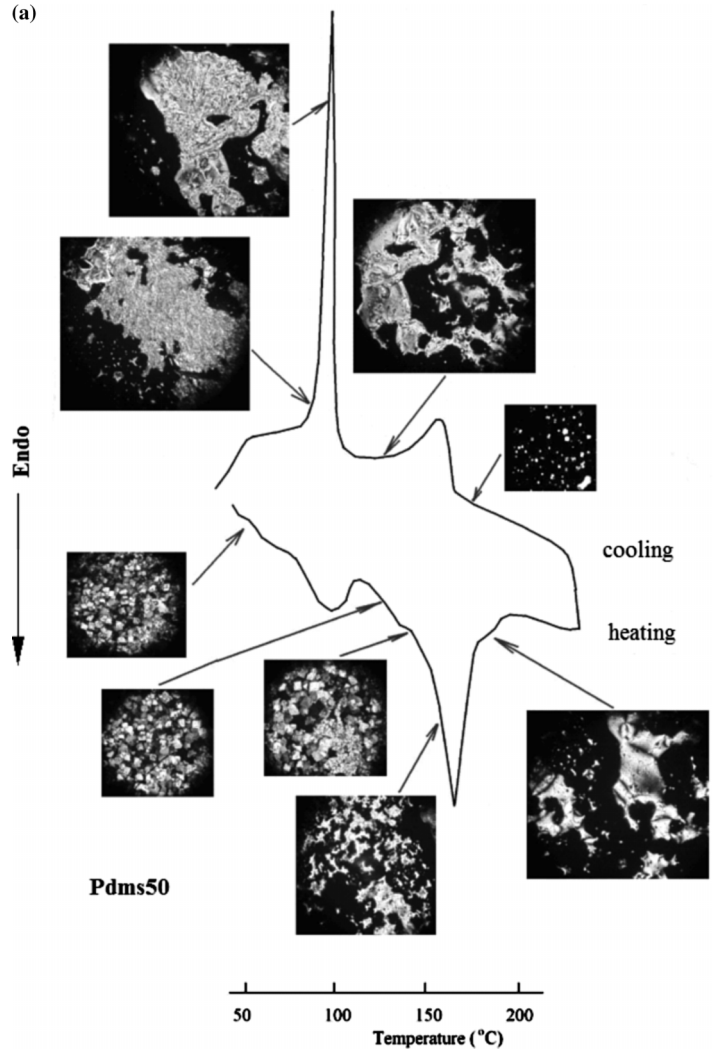

Figure 2. Combination of DSC curves and POM images of (a) Pdms50, (b) PdmsE50 and (c) PSF20 upon heating and consequent cooling.

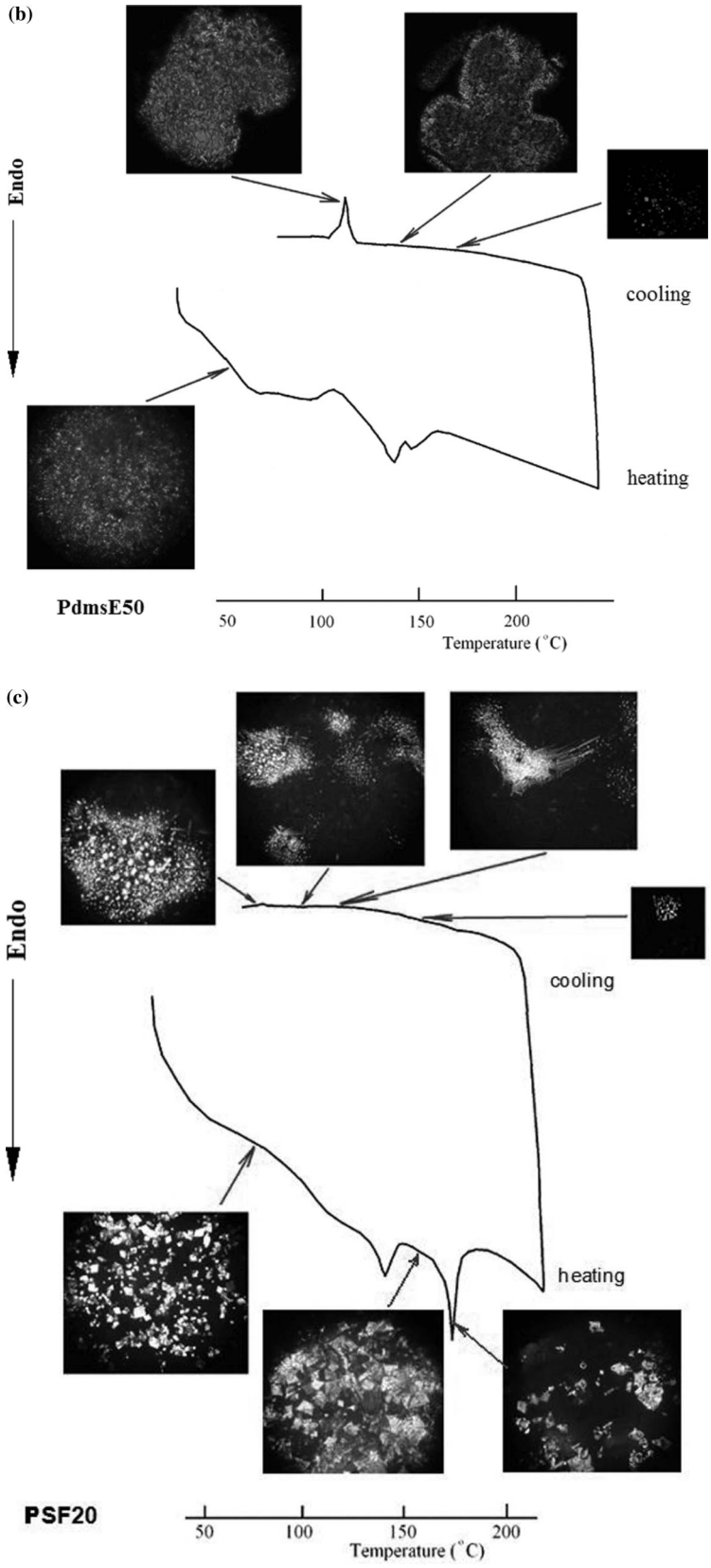

Figure 2. (*Continued*)

Typical behaviour of the PDLCs with the PSF matrix is exemplified in Figure 2(c) for PSF20. Apart from the polymer T_g, the DSC curve showed the melting of the LC phase at 140°C and another peak at 175°C; no noticeable transition was detected upon cooling, probably due to the increased miscibility achieved in the molten state. According to the POM data, the crystals melted at 140°C into a smectic mesophase, which became isotropic at 185°C. Upon cooling, the LC droplets appeared at 165°C and maintained their shape during further observation.

As can be seen from the previous observations, there is no perfect correlation between the two methods DSC and POM, because of the difference in heating and cooling rates and also because of the difference in the measurement principles. Nevertheless, our main interest in this research was in a specific, i.e. I–N, transition.

Figure 3 shows the fragments of the typical texture images observed microscopically across the thermally induced I–N phase transition in Pdms80, PdmsE80 and PSF80. Bright areas of a nearly circular form relate to the nematic phase, whereas black background refers to the isotropic phase, i.e. the nematic phase appears within the dispersed LC phase, where it is stabilised and supported by the solid polymer matrix. The results of the statistical treatment of the selected images in the form of histograms are presented in Figure 4. Their analytical description by Equation (1) with the fitting parameters listed inside the boxes is also given in Figure 4 in the form of solid lines. The successful description evidently indicates that nematic droplets form a singular thermodynamically optimised statistical ensemble across the phase transition (*22*, *23*).

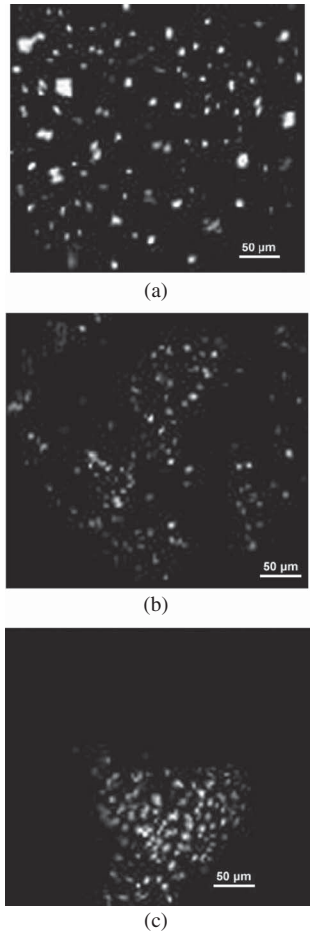

Figure 3. POM images of (a) Pdms80, (b) PdmsE80 and (c) PSF80 across the I–N phase transition at (a) 80s, (b) 95s and (c) 65s after beginning of the phase separation.

In Figure 5 the mean droplet diameter, being computed with Equations (2) and (3), is presented as a function of time. In our previous studies related to the phase separation in non-confined azomethine LCs of different molecular weights (from monomers to polymers), we observed two regimes of the ordered phase evolution, i.e. nucleus growth and nucleus coarsening, across the phase transition (*14*, *15*, *19*, *20*). Conversely, in the present investigation only the nucleus growth regime can be seen. We observed a weak coalescence at $t > 50$ s for Pdms50 and Pdms80 only. We can therefore conclude that the confined geometry of LCs prevents the droplet coalescence, since the polymer matrix segregates one LC droplet from another, not allowing them draw closely for their coarsening.

For the analytical description of the nematic phase growth presented in Figure 5 we used the following equation of the phase ordering kinetics (*16*)

$$<d> = ct^n \tag{4}$$

with the growth exponent value $n = 1/2$, being typical for systems with a non-conserved order parameter (*16*). The results of computation are shown in Figure 5 as solid lines.

As follows from Figure 5, the mean droplet diameter, in fact, does not change significantly after 100s. We accepted this $<d>$ value as the saturated value, $<d_{sat}>$, and plot it as a function of the LC concentration in PDLCs. This presentation is given in Figure 6.

Figure 6 allows elucidation of the influence of the polymer matrix nature on kinetics of the nematic phase growth. No significant change in the $<d_{sat}>$ values is seen at increasing concentration of LC component in the LC/Pdms system. Indeed, the Pdms matrix can be treated as a 'soft' matrix since it is fluid across the LC component phase transition and can be 'expanded' with increasing concentration of LC component without any mechanical hindrance from the polymer

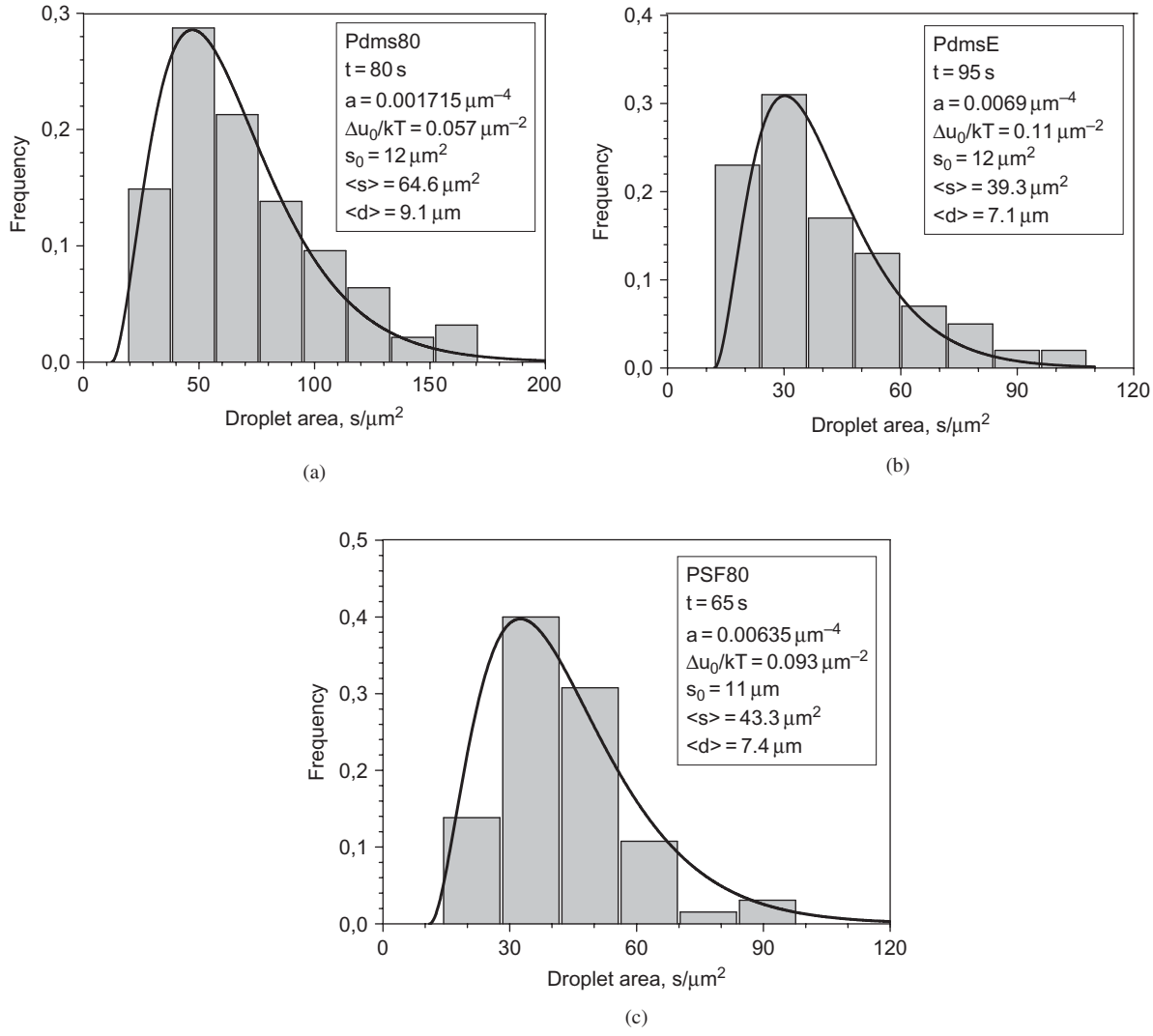

Figure 4. Statistical area distributions of the nematic droplets depicted in Figure 3 and their description using Equation (1) with the fitting parameters listed within the boxes, where the mean droplet area and the mean droplet diameter computed with Equations (2) and (3) are also given.

matrix. Besides, according to the DSC data mentioned above, T_g of Pdms does not change irrespectively to the LC concentration (−123.5°C). This means that PDLC of this type can be treated as a two-phase mixture demonstrating incompatibility and independence in behaviour of its components, i.e. the LC component and the Pdms matrix.

In the LC/PdmsE system, $<d_{sat}>$ decreases noticeably with concentration, presumably in a linear manner. The PdmsE matrix can rather be considered as a 'semi-flexible' matrix since it is, in fact, the same polymer as mentioned above but subjected to cross-linking under curing with TEOS and DBTDL. It has a restricted mobility and presents a decrease in the LC droplet size at the increasing LC phase concentration, since the number of droplets becomes too much at high concentration, and this prevents their growth because of geometrical restriction.

However, the PSF matrix should be treated as the most 'rigid' matrix, due to its chemical structure. This restricts the nematic phase growth even at low concentration of the LC phase and the further increase in the LC concentration decreases the $<d_{sat}>$ values a little. According to the DSC data, T_g = 185°C for PSF decreases seriously after the LC component embedding (Table 1). This indicates a good mixing and plasticising effect of the LC component involved. Both effects can explain the existence of the smaller droplets and also a small difference between the samples with the increasing LC concentration.

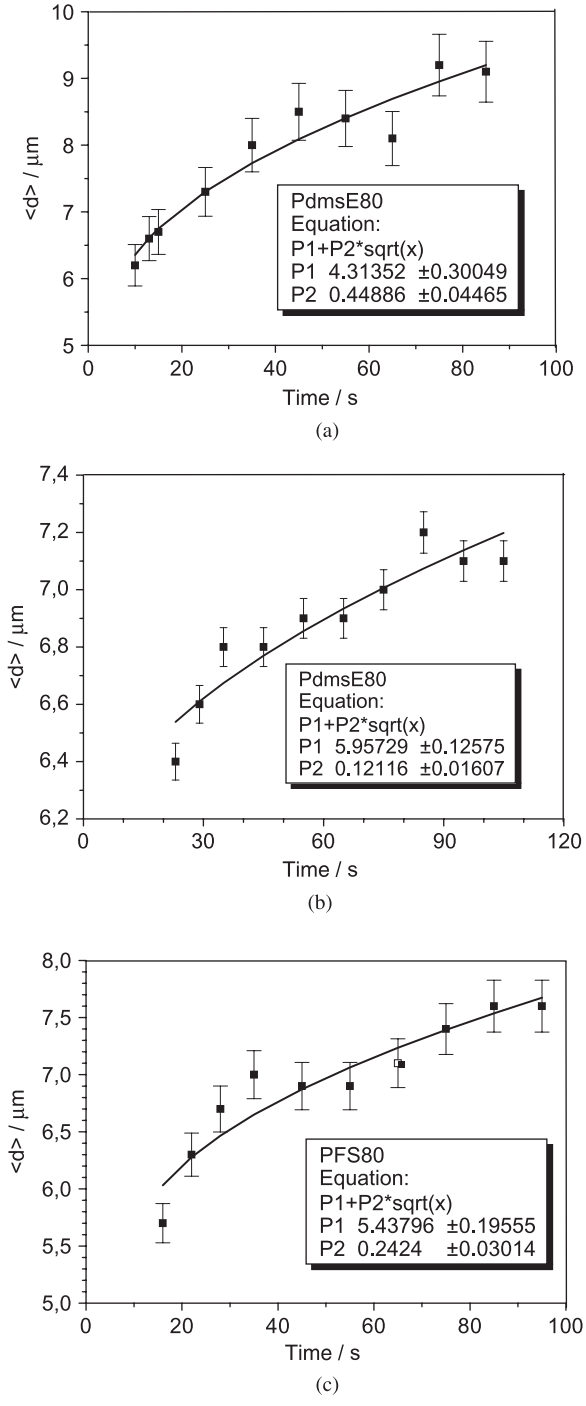

Figure 5. Evolution of the mean droplet diameter with time across the I–N phase transition in (a) Pdms80, (b) PdmsE80 and (c) PSF80.

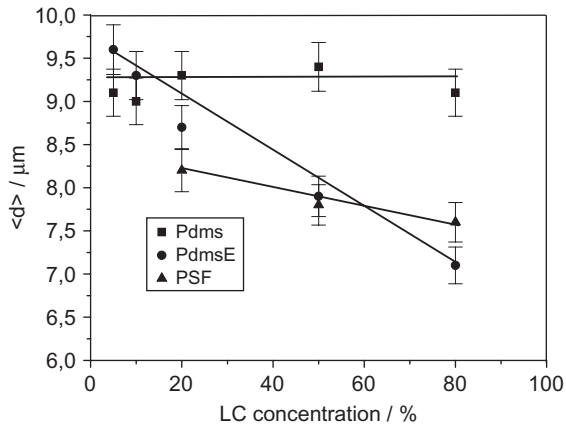

Figure 6. Saturated mean droplet diameter versus the LC phase concentration in (a) Pdms80, (b) PdmsE80 and (c) PSF80.

5. Conclusions

PDLCs composed of 'soft' (Pdms), 'semi-flexible' (PdmsE) and 'rigid' (PSF) matrices and an azomethine mesogen compound were prepared by combination of SIPS and TIPS. The analysis of the thermal behaviour of the PDLCs detected by DSC and POM methods upon heating and cooling allowed us to conclude that the phase behaviour of the LC compound was significantly affected by both the nature of the polymer matrix and the composition of the PDLCs.

We paid particular attention to the kinetics of the nematic phase growth across the I–N phase transition upon cooling the PDLC melt. Statistical analysis of the POM images allowed us to conclude that the nematic droplets form thermodynamically optimised statistical ensembles, where the mean droplet diameter increases proportionally to square root of time.

The influence of the mesogen content and the matrix flexibility/rigidity on the kinetics of the nematic phase growth was clarified when we analysed the saturated values of the droplet diameter. We can deduce:

(1) In the LC/Pdms system, both components are immiscible across the I–N phase transition and this 'soft' polymer matrix does not prevent the nematic phase growth. That is why, in these PDLCs, $<d_{sat}>$ does not depend on the LC phase concentration.
(2) In the LC/PdmsE system, a 'semi-flexible' polymer matrix restricts the growth of nematic droplets when concentrations of the LC phase increases. That is why $<d_{sat}>$ decreases significantly with the LC phase concentration.
(3) In the LC/PSF system, the components are miscible and this 'rigid' matrix hinders the growth of nematic droplets. That is why $<d_{sat}>$ is smaller and decreases a little with the LC phase concentration.

References

(1) Doane, J.W. In *Liquid Crystals: Applications and Uses*, Bahardur B., Ed.; World Scientific: Singapore, 1990.

(2) Drzaic, P.S. *Liquid Crystal Dispersion*. World Scientific: Singapore, 1995.
(3) Jeon, Y.J.; Bingzhu, Y.; Rhee, J.T.; Cheung, D.L.; Jamil, M. *Macromol. Theory Simul.* **2007**, *16*, 643–659.
(4) Carter, S.A.; LeGrange, J.D.; White, W.; Boo, J.; Wiltzius, P. *J. Appl. Phys.* **1997**, *81*, 5992–5999.
(5) Amundson, K.; van Blaaderen, A.; Wilzius, P. *Phys. Rev. E* **1997**, *55*, 1646–1665.
(6) Han, J.-W. *J. Korean Phys. Soc*. **2006**, *49*, 563–568.
(7) Chen, L.G.; Shanks, R. *Liq. Cryst*. **2007**, *34*, 1349–1356.
(8) Tercjak, A.; Serrano, E.; Larrañaga, M.; Mondragon, I. *J. Appl. Polym. Sci.* **2008**, *108*, 1116–1125.
(9) Pierron, J.; Tournier-Lasserve, V.; Sopena, P.; Boudet, A.; Sixou, P.; Mitov, M. *J. Phys. II France*, **1995**, *5*, 1635–1647.
(10) Justice, R.S.; Schaefer, D.W.; Vaia, R.A.; Tomlin, D.W.; Bunning, T.J. *Polymer* **2005**, *46*, 4465–4473.
(11) Lucchetti, L., Simoni, F. *J. Appl. Phys.* **2000**, *88*, 3934–3940.
(12) Motoyama, M.; Nakazawa, H.; Ohta, T.; Fujisawa, T.; Nakada, H.; Hayashi, M.; Aizawa, M. *Comp. Theor. Polym. Sci.* **2000**, *10*, 287–297.
(13) Xia, J.; Wang, J.; Lin, Z.; Qiu, F.; Yang, Y. *Macromolecules* **2006**, *39*, 2247–2253.
(14) Bronnikov, S.; Dierking, I. *Phys. Chem. Chem. Phys*. **2004**, *6*, 1745–1749.
(15) Bronnikov, S.; Nasonov, A.; Racles, C.; Cozan, V. *Soft Mater*. **2008**, *6*, 119–128.
(16) Bray, A.J. *Adv. Phys.* **2002**, *51*, 481–587.
(17) Diekmann, K.; Schumacher, M.; Stegenmeyer, H. *Liq. Cryst.* **1998**, *25*, 349–355.
(18) Dierking, I. *J. Phys. Chem. B* **2000**, *104*, 10642–10646.
(19) Bronnikov, S.; Racles, C.; Nasonov, A.; Cazacu, M. *Liq. Cryst.* **2006**, *33*, 1015–1019.
(20) Bronnikov, S.; Cozan, V.; Nasonov, A. *Phase Transit*. **2007**, *80*, 831–839.
(21) Alexandru, M.; Cristea, M.; Cazacu, M.; Ioanid, A.; Simionescu, B.C. *Polymer Composites*, **2008**, Doi: 10.1002/pc.20608
(22) Kilian, H.G.; Metzler, R.; Zink, B. *J. Chem. Phys.*, **1997**, *107*, 8697–8705.
(23) Kilian, H.G.; Bronnikov, S.; Sukhanova, T. *J. Phys. Chem. B*, **2003**, *107*, 13575–13582.
(24) Mark, J.E., Ed. *Polymer Data Handbook*, Oxford University Press: New York, 1996.
(25) Bicerano, J. *Prediction of Polymer Properties*, 3rd Ed., Marcel Dekker: New York-Basel, 2002.
(26) Hansen, M. *Ind. Eng. Chem., Prod. Res. Dev*. **1969**, *8*, 2–11.